Title
DOUBLE PERIPHERAL MODEL ANALYSIS OF THE REACTION K+p-^K+rt- A. JLg AT 9 GeV/c

Author
Fu, Chumin.

Publication Date
1970-06-01

Submitted to Physical Review

UCRL-19807
Preprint

c. 2

DOUBLE PERIPHERAL MODEL ANALYSIS OF THE REACTION $K^+p \to K^+\pi^-\Delta^{++}_{1236}$ AT 9 GeV/c

Chumin Fu

June 1970

AEC Contract No. W-7405-eng-48

LAWRENCE RADIATION LABORATORY
UNIVERSITY of CALIFORNIA BERKELEY

DISCLAIMER

DOUBLE PERIPHERAL MODEL ANALYSIS OF THE REACTION $K^+p \to K^+\pi^- \Delta^{++}_{1236}$ AT 9 GeV/c

Chumin Fu

Lawrence Radiation Laboratory
University of California
Berkeley, California 94720

ABSTRACT

Using a double Regge-pole-exchange model, we studied the low $\Delta^{++}\pi^-$ mass enhancement in the reaction $K^+p \to K^+\pi^-\Delta^{++}_{1236}$ at 9 GeV/c. We found that P and π double exchange dominate the process. In general the model agrees with the data in the region where $M(K^+\pi^-) \gtrsim 1.54$ GeV and $-t_{KK} < 0.5$ (GeV/c)^2 and $-t_{p\Delta} < 0.5$ (GeV/c)^2. The possibility of extending the model into the large t region and problems involved in the extrapolation of the model to the $K\pi$ threshold are investigated. The importance of the contribution from the double peripheral process in low $M(K^+\pi^-)$ region and its implications to the analysis for the $K\pi$ system are discussed.

I. INTRODUCTION

The general features of the reaction $K^+p \to K^+\pi^-\Delta^{++}_{1236}$ at 9 GeV/c were discussed in an earlier communication.[1] In this paper we study the reaction in the high $k\pi$ mass region ($M(K^+\pi^-) \gtrsim 1.54$ GeV) on the basis of a double Regge-pole-exchange model. The advantage of this model is that it has the same simple form as a single Regge-pole-exchange model and theoretically the Regge parameters (except the coupling at the internal vertex) used here can be wholly taken from those that were determined by the data from two-body or quasi-two-body final states. As a known fact, a double-Regge-pole model can usually describe the data of the three-body or quasi-three-body final states at high energies fairly well. However, in applying the model, there are still some unsolved problems; namely,

1) The commonly used Regge parameters are known only to their order of magnitude. The exact values are not well determined. Hence when one finds that the fits of the model to the data are insensitive to the variation of the parameters, one cannot distinguish whether it is due to the effect of a collective change of the many Regge parameters or due to an incomplete study of the data. Poor statistics of the data and unclean samples could also contribute to the sources of uncertainties.

2) There is no evidence for Toller angular dependence at the internal vertex. By the same argument given in 1) above, it is not clear at all whether or not there should be a Toller angular dependence for the Reggeon-Reggeon-particle coupling.

3) How far in momentum transfer variables (t's) a peripheral model can extend is not well known.

4) Granted that the duality is a valid concept,[2]

how would one extrapolate the model to small subinvariant energies (s's)? Would the extrapolation be insensitive to the variation of Regge parameters also? Answers to these questions are not known either.

With an attempt to understand these problems we analyze our data in an exhaustive manner. The method and the results of the analysis are presented in Secs. II and III. Section IV discusses the extrapolation of the model to small subinvariant energies. Section V gives our conclusions.

This experiment was carried out in the Brookhaven National Laboratory 80-inch hydrogen bubble chamber, which was exposed to a 9-GeV/c rf-separated K^+ beam at the AGS. The details of the experiments, the measurements, and the kinematical fitting procedures are described in Ref. 1 and the Ref. 5 therein.

II. THE MODEL AND THE METHOD OF ANALYSIS

A. The Model

There are many multiperipheral models and the phenomenological analyses of the data discussed in the literature.[3,4] Here we adopt the one given in Ref. 3c. Consider Fig. 1a, a diagram for the reaction $a + b \to 1 + 2 + 3$. The invariant amplitude is

$$A(s, s_1, s_2, t_1, t_2) \approx \beta_1(t_1)\,\xi_1(t_1)\left(\frac{\tilde{s}_1}{s_{10}}\right)^{\alpha_1(t_1)} \times \beta_2(t_2)\xi_2(t_2)\left(\frac{s_2}{s_{20}}\right)^{\tilde{\alpha}_2(t_2)} \beta_3(t_1, t_2, \omega), \qquad (1)$$

where s, s_1, s_2, and t_1 and t_2 are as indicated in Fig. 1a.

$$\tilde{s}_1 = s_1 - t_2 - m_a^2 + \tfrac{1}{2} t_1^{-1}(m_1^2 - m_a^2 - t_1)(m_3^2 - t_1 - t_2)$$

and $\tilde{s}_2$ is obtained by interchanging the subscripts 1 and 2. The Toller angle, ω, is defined by

$$\cos\omega = \frac{\vec{p}_a \times \vec{p}_1 \cdot \vec{p}_b \times \vec{p}_2}{|\vec{p}_a \times \vec{p}_1|\,|\vec{p}_b \times \vec{p}_2|}$$

in the rest frame of the particle 3. The α_i's are the Regge trajectories exchanged and

$$\xi_i = \frac{1 \pm e^{-i\pi\alpha_i(t_i)}}{\sin \pi\alpha_i(t_i)}.$$

The β_i's are the residue function. The s_{i0}'s are the energy scale constants.

For the reaction $K^+p \to K^+\pi^-\Delta^{++}_{1236}$, the allowable exchange pairs (α_1, α_2) are (P, π), (P, A_1), (ρ, π), (ρ, A_2), (ρ, A_1) and (ω, ρ). Consider the (P, π) pair only and further assume that P is a fixed pole with an intercept 1 in the Chew-Frautschi plot. After squaring Eq. (1) and some simplifications one obtains an intensity

$$I = N_0 e^{\gamma t_1} \frac{(\pi\alpha'_\pi)^2}{1 - \cos\pi\alpha_\pi(t_2)} (\tilde{s}_1)^2 \left(\frac{\tilde{s}_2}{s_0}\right)^{2\alpha_\pi(t)} f(\omega, t_1, t_2), \qquad (2)$$

where $\alpha_\pi = \alpha'_\pi(t_2 - m_\pi^2)$ and N_0 is a normalization constant. This equation is the same as that given in Ref. 3e provided that we set $f(\omega, t_1, t_2)$ to be constant.

Since Pomeranchukon is not well understood at present and there are five exchange pairs other than (P,π) also allowed, for $K^+\pi^-$ mass between 1.54 and 2.8 GeV it is reasonable to replace $(\tilde{s}_1)^2$ by $(s_1)^{2c}$ in Eq. (2), where c is a constant parameter.

Using the notations indicated in Fig. 1b, we rewrite Eq. (2) as

$$I = N_0 e^{\gamma t_{KK}} \frac{(\pi\alpha_\pi)^{2c}}{1 - \cos\pi\alpha_\pi(t_{p\Delta})} (\tilde{s}_{K\pi})^{2c} \left(\frac{\tilde{s}_{\Delta\pi}}{s_0}\right)^{2\alpha_\pi(t)} \times f(\omega, t_{p\Delta}, t_{KK}), \qquad (3a)$$

which is to be used in this analysis. We assume that f takes the form

$$f = [1 + a(t_{p\Delta}/m_\pi^2)\cos\omega]^2, \qquad (3b)$$

where a is a constant parameter. Equation (3b) is purely empirical. It has the property that f has no Toller angular dependence at $t_{p\Delta} = 0$, which is required on a theoretical basis.[4] In this analysis, there are five

parameters involved, i.e., γ, α'_π, c, s_0 and a. Two cases are considered, namely

1) Case I: a = 0,
2) Case II: a is a free parameter.

B. The Method of Analysis

In comparing the data with the theoretical calculations we follow the procedures below:

1) Generate Monte Carlo events for the $K^+\pi^-\Delta^{++}_{1236}$ final states with a variable mass for the Δ^{++}_{1236} given by a Breit-Wigner distribution.[6]

2) Assign to each Monte Carlo event a weight according to Eq. (3a).

3) Compare the various distributions from the Monte-Carlo events with those from the data, and vary the parameters in Eq. (3a) until we obtain the best fit for all those distributions considered. The goodness of the fit is determined by a χ^2 calculation.[7]

In order to investigate the problems stated in the introduction, we choose to study the following three samples with $M(K^+\pi^-) > 1.54$ GeV:

Sample A: $-t_{K^+K^+}$ and $-t_{p\Delta^{++}} < 1.0$ $(GeV/c)^2$ (511 events).

Sample B: $-t_{K^+K^+}$ and $-t_{p\Delta^{++}} < 0.5$ $(GeV/c)^2$ (287 events).

Sample C: $-t_{K^+K^+}$ and $-t_{p\Delta^{++}} < 0.3$ $(GeV/c)^2$ (115 events).

The N_0 is determined by normalizing to sample B the Monte Carlo events with the same kinematic cuts as those imposed on sample B. The parameters γ, α'_π, c, s_0, and a are obtained by comparing the distributions of 12 variables from the events in sample B with those from the corresponding Monte Carlo events [three invariant masses, $M(K^+\pi^-)$, $M(\Delta^{++}\pi^-)$, and $M(K^+\Delta^{++})$, four four-momentum transfers, $-t_{KK}$, $-t_{p\Delta}$, $-t_{K\pi}$, and $-t_{p\pi}$, and five angular variables, $\cos\theta(K^+\pi^-)$, $\phi(K^+\pi^-)$, $\cos\theta(\Delta^{++}\pi^-)$, $\phi(\Delta^{++}\pi^-)$, and ω]. The θ and ϕ are the Jackson angle and the Treiman-Yang angle for a two-particle composite. If the model is valid and the parameters obtained are correct, then one should expect good agreements between the various distributions from the Monte Carlo events and those from the data in a t region where the t cuts are smaller than what sample B has. Furthermore one can also test the validity of the model in a large t region by extending the t cuts imposed on the data and the Monte Carlo events. These are the motivations for studying samples C and A. In principle one should compare the model with the data in different noninclusive t intervals. Due to the statistical limitations of our data, we can only choose the t criteria as we described earlier.

III. RESULTS

Various values for the parameters in Eq. (3a) have been tried; the best values obtained are

Case I: a = 0, $\gamma = 4$ $(GeV/c)^{-2}$, $\alpha'_\pi = 1.2$ $(GeV/c)^{-2}$, $s_0 = 1.0$ $(GeV)^2$, and c = 0.85

Case II: a = 0.015, $\gamma = 3.2$ $(GeV/c)^{-2}$, $\alpha'_\pi = 1.12$ $(GeV/c)^{-2}$, $s_0 = 1.0$ $(GeV)^2$, and c = 0.85.

A. The Distributions of the Various Kinematic Variables

For each variable the distributions are to be presented in the order of Samples A, B, and C. The corresponding distributions from the Monte Carlo events are shown in solid lines for case I and long dash lines for case II.

Figure 2 shows the Δ^{++}_{1236} mass distributions. Here we check whether the Monte Carlo events generated for the $K^+\pi^-\Delta^{++}_{1236}$ final state indeed have a $p\pi^+$ mass distribution similar to that of the samples. Comparing the data with the curve shown in Fig. 2b, we obtain a $\chi^2 = 16.4$ and a confidence level = 12.6% with 14 degrees of freedom. (We consider M_0, Γ_0, and a as parameters in the Breit-Wigner distribution discussed in Ref. 6. The curves

corresponding to case I and case II are very close, therefore only the result of case I is shown in Fig. 2.)

Figure 3a, b, and c shows the $K^+\pi^-$ mass spectra for samples A, B, and C respectively. The short-dash lines are the extrapolations of the model calculations to the region where $M(K^+\pi^-) < 1540$ MeV. Discussions of the extrapolation are given in Sec. IV. In Fig. 3b the two curves are close in the region where $M(K^+\pi^-) \gtrsim 1700$ MeV. Below 1700 MeV in the $K^+\pi^-$ mass two curves start to deviate. The deviation between the solid and the long dash lines become larger for sample A and smaller for sample B. This seems to be a general trend shown also in the other distributions we discuss later.

Figures 4a, b, and c and Figs. 4d, e, and f show the $\Delta^{++}\pi^-$ mass distributions and the $K^+\Delta^{++}$ mass distributions. In Fig. 4a the data peak at around 1500 MeV, where there are three I = 1/2 baryonic resonances, P_{11}, D_{13}, and S_{11}.[8] The calculated curves peak at about 80 MeV above 1500 MeV. However, in Figs. 4b and c the curves agree with the data. The curves from the model shift their peak by 80 MeV in the $\Delta^{++}\pi$ mass from Fig. 4a to Figs. 4b and c, yet the data do not show such an apparent change. This indicates that the model may very well apply to small t regions (e.g., samples B and C) but does not apply to the large t regions (e.g., sample A). Similar disagreements also show some of the distributions from sample A discussed in the following paragraphs. In Fig. 4d the dashed curve agrees with the data better than the solid curve, but it is not so obvious in Figs. 4e and f.

Figures 5 and 6 show the distributions of $-t_{KK}$ and $-t_{p\Delta}$, and $-t_{K\pi}$ and $-t_{p\pi}$. Except for $-t_{p\pi}$ in Fig. 6e and f, in general the model (for both case I and case II) agrees well with the data.

Figure 7 shows the decay angular distributions for the $K^+\pi^-$ system in its rest frame. The $\cos\theta$ distribution (Figs. 7a, b, and c) are plotted from 0 to 1.0 since there are no events from the data and the model in the backward region. As the t cuts decrease, the events are populated even in a smaller forward region [e.g., $\cos\theta(K^+\pi^-) \geq 0.7$ for both $-t_{KK}$ and $-t_{p\Delta}$ less than 0.3 $(GeV/c)^2$]. The Treiman-Yang angular distribution (Figs. 72, f, and g) becomes flatter as $t_{p\Delta}$ decreases. This indicates that the Treiman-Yang angular distribution tends to agree with the well-known prediction of single-pion particle exchange in the limit of very small $-t_{p\Delta}$.[9] The solid curve and the dashed curve show considerable discrepancy in Fig. 7d (sample A). Otherwise, for both case I and case II the model agrees with the data rather well.

Figure 8 shows the distributions of the $\cos\theta$ and ϕ for the $\Delta^{++}\pi^-$ system. Again a large discrepancy between the curves is observed in large t regions (Figs. 8a and d). Figure 9 shows the Toller angular distributions. The model agrees with the data fairly well for Sample B, but does not agree with the data in both the large t region (sample A) and the small t region (sample C). The dash-dot lines in Fig. 9 represent the phase space which is normalized to each sample. It strongly peaks near ω = 180 deg. At ω = 180 deg, the two particles in the initial state and the three particles in the final state lie in the same plane. As t cuts decrease, the phase space curve is getting closer to the results of the model and the data points.

The χ^2 values of the various distributions for sample B are given in Table I. Table I indicates:

1) Over all the kinematical variables studied the confidence level of case II is more uniform than that of case I. Consider the latter if one happens to choose to fit the distributions of $M(K^+\pi^-)$, $M(K^+\Delta^{++})$, $-t_{p\Delta}$, and $-t_{K\pi}$ one may claim very good agreement between the model and the data. On the other hand if one chooses the variables $M(\Delta^{++}\pi^-)$, $-t_{KK}$, $-t_{p\pi}$, and the

Toller angle, ω, one may consider that the model is a failure. The results could be even worse if only some of the distribution from sample A were considered.

2) The agreement between the model and the data is poor for the distributions of $-t_{KK'}$, $-t_{p\pi'}$ and ω.

B. A Quantitative Analysis

Comparison of the number of events from the model and the phase space with the data under different kinematical criteria is shown in Table II. The normalization was described in Sec. IIB.

We observe the following:

1) Comparing the numbers from the data and those from the phase space, one can easily see the peripheral nature of the data.

2) For $M(K^+\pi^-) \geq 1540$ MeV, the number of events from the data agrees with the result of the model for both case I and case II. The model completely disagrees with the data in the low $K^+\pi^-$ mass region [$M(K^+\pi^-) < 1540$ MeV] as we expect (because of the strong K^* resonance productions). One important point to note is that the predictions of case I and case II disagree in this $K^+\pi^-$ mass region also.

IV. EXTRAPOLATION OF THE MODEL TO SMALL SUBENERGIES

In this section we discuss: (a) the importance of the contribution from the extrapolation, (b) the reliability of the extrapolation with the present knowledge of Regge parameters, and (c) the isospin structure of the $K\pi$ system on the basis of (P, π) exchange in the model.

(a) In order to demonstrate the contribution from the double peripheral process by extrapolation, in Figs. 10a, b, and c we plot the complete $K^+\pi^-$ mass spectra under the t cuts, $-t_{KK}$ and $-t_{p\Delta}$ less than 1.0 $(GeV/c)^2$, 0.5 $(GeV/c)^2$, and 0.3 $(GeV/c)^2$ respectively. The curves shown in Figs. 10a, b, and c are the same as those shown in Figs. 3a, b, and c. The extrapolation of the model to the small $K\pi$ mass region as shown by the dashed curves in Fig. 10 does not describe the data in the K^*_{890} resonance region, not in a crude average sense. This seems to be in favor of Harari postulate[10] that Pomeranchukon exchange is responsible for the background only. The double peripheral process would contribute at least 30 to 60% of the background in the low $K\pi$ mass region [$M(K^+\pi^-) < 1540$ MeV]. Due to the $e^{\gamma t_{KK}}$ factor in Eq. (3a), the model yields a large intensity in the forward $\theta(K^+\pi^-)$ region even in the low $K\pi$ mass region (except near the $K\pi$ threshold). This contributes to part of the well-known forward-backward asymmetry in the $K\pi$ system.[11] Ignoring the isospin structures, calculations involving a p-wave K^*_{890} and a d-wave K^*_{1420} with a coherent and an incoherent double peripheral process with (P, π) exchange have been tried. They do not produce some of the important features in $K\pi$ asymmetry as a function of $K\pi$ mass. Since the contribution from the extrapolation to the background is large and yet it cannot account for all the background beside the two well-established K^*'s, one may ask whether the double peripheral process or the K^* resonance productions can be isolated from the data in order to obtain a relatively clean sample. The answer to this question is no, because both processes are dominated by pion exchange and in favor of small $-t_{p\Delta}$.

(b) In Table II the numbers of events in the low $K\pi$ mass region from the extrapolation of the model differ by about 30% between case I and II. This is a typical fluctuation, introduced to a certain extent by the uncertainties of the parameters used in Eq. (3a). With the present knowledge about Regge parameters and the statistical level of the data, one cannot determine how much each exchange pair (discussed in Sec. IIA) contributes, or whether one should try to find a better new model. Hence at the present stage the extrapolation of the model can

only offer a qualitative description for the data.

(c) Based on an isospin argument in Ref. 1 it was concluded that the low $\Delta^{++}\pi^-$ mass enhancement is predominately of I = 1/2. This isospin assignment is in favor of an I = 0 object exchanged at the $K^+_{in}K^+_{out}$ vertex. Among all the allowed exchange pairs (see Sec. IIA) the P is the only candidate with I = 0.

In fact we obtain $C \approx 0.85$, which is close to unity, in this analysis. This agrees with the assumption that P is the dominant object exchanged at the K^+K^+ vertex. Comparing (P, π) and (P, A_1), if one assuming α_π and α_{A_1} have the same slope, then A_1 would be a lower trajectory and its pole is farther away from the physical region than the pion pole. Hence the contribution of A_1 is less important than that of π. If one assumes π and A_1 degeneracy then there should be no essential difference whether (P, A_1) is included or not in addition to (P, π). The comparison of the model and the data also indicates that our (P, π) assumption is rather good at least in the region where $-t_{KK}$ and $-t_{p\Delta}$ are small. These arguments justify the assumption that the (P, π) exchange pair dominates the double peripheral process. Then one can further study the upper part of the diagram in Fig. 1b as a K^+_{in} scattered by a virtual pion producing the $K^+\pi^-$ final state with P exchanged in the t channel. By isospin crossing,[12] for the reaction $K^+\pi^- \to K^+\pi^-$ via an I = 0 object exchanged in the t channel, the I = 3/2 and I = 1/2 parts of the amplitude are in 1:2 ratio. The implications of this is that we cannot neglect the I = 3/2 component in doing analysis for the $K\pi$ system in low $K\pi$ mass region. Whether the $K\pi$ asymmetry can be explained by including the I = 3/2 component is completely unclear.

V. CONCLUSIONS

1. (P, π) exchange dominates the reaction $K^+p \to K^+\pi^-\Delta^{++}_{1236}$ at 9 GeV/c for $M(K^+\pi^-) \geq 1540$ MeV. In general the model agrees with the data fairly well for $-t_{KK} < 0.5$ $(GeV/c)^2$ and $-t_{p\Delta} < 0.5$ $(GeV/c)^2$. The validity of the model above these t cuts is definitely in doubt.

2. The introduction of an empirical Toller angular dependence at the internal vertex helps to improve the condifence level to be more uniform over the distribution of all the variables considered except that the fit to the Toller angular distributions itself has not been improved much. In the small t region, the Toller angular distribution (as shown in Fig. 9c) indicates a large discrepancy between the model and the data. Further investigation on Toller angular dependence is necessary.

3. With the present knowledge of the Regge parameters determined by the data from two-body final states, the many possibilities of the exchange pairs, and the statistical limitation of our data, the values of the Regge parameters we used are subject to considerably large uncertainties. However, this should not affect the conclusion that the contribution from the extrapolation is large. By comparing the data with the result from the extrapolation to small $K\pi$ mass region, we find that the latter agrees with Harari's postulate that Pomeran exchange is responsible for the background only.

ACKNOWLEDGMENTS

I would like to acknowledge Professor G. Goldhaber, Dr. E. L. Berger, Dr. A. Firestone, and Dr. P. D. Ting for their critical comments and discussions. I thank Dr. R. Shutt and the staff of the 80-inch bubble chamber and Dr. H. Foelsche and the AGS staff at Brookhaven for helping with the exposure. I am also thankful for the valuable support given by the White and the FSD staff and by our programming and scanning staff, in particular Emmett R. Burns.

FOOTNOTE AND REFERENCES

*Work supported by the U. S. Atomic Energy Commission.

1. C. Fu, A. Firestone, G. Goldhaber, and G. H. Trilling, Nucl. Phys. B18, 93 (1970).

2. a) R. Dolen, D. Horn, and C. Schmid, Phys. Rev. 166, 1768 (1968).

b) G. F. Chew and A. Pignotti, Phys. Rev. Letters 20, 1078 (1968).

3. a) N. F. Bali, G. F. Chew, and A. Pignotti, Phys. Rev. Letters 19, 614 (1967) and Phys. Rev. 163, 1572 (1967).

b) Chan Hong-Mo, K. Kajantie, and G. Ranft, Nuovo Cimento 49, 157 (1967) and E. Flamino, Nuovo Cimento 51, 696 (1967).

c) Review talks given by Chan Hong-Mo and S. Ratti in Topical Conference on High-Energy Collisions of Hadrons, CERN, January 1968.

d) Review talks by Chan Hong-Mo and O. Czyzewski, in Proceedings of the 14th International Conference on High-Energy Physics, Vienna, 28 August-5 September, 1968 (CERN, 1968).

e) Review talk given by J. D. Jackson, in Proceedings of the Lund International Conference on Elementary Particles, Lund, Sweden, June 25-July 1, 1969 (Berlingska Boktryckeriet Lund, Sweden, 1969).

f) G. Ranft, Fortschr. Physik (in press).

g) E. L. Berger, Phys. Rev. 179, 1567 (1969).

4. Double peripheral model analyses on $K\pi\Delta^{++}$ final states; see:

a) G. Bassompierre et al., Nucl. Phys. B14, 143(1969) on the reaction $K^+p \to K^+\pi^-\Delta^{++}$ at 5 GeV/c.

b) J. Andrews, J. Lach, T. Ludlam, J. Sandweiss, H. D. Taft, and E. L. Berger, Phys. Rev. Letters 22, 731(1969) on the reaction $K^-p \to K^-\pi^-\Delta^{++}$ at 12.6 GeV/c.

Many phenomenological analyses on the other reactions were reviewed in references 3(b), (c), (d), and (e).

5. J. M. Kosterlitz, Nucl. Phys. B9, 273 (1969).

6. A. Breit-Wigner distribution of the form $M_0\Gamma/[M_0^2 - M)^2 + \Gamma^2 M_0^2]$ with $\Gamma = (\Gamma_0/M)(p/p_0)^3 (am_\pi^2 + p_0^2)/(am_\pi^2 + p^2)$ is used. The M is the $p\pi^+$ invariant mass. The M_0 is the mass of M at resonance. The p and p_0 are the momenta of the proton in the $p\pi^+$ cm system at a mass M and M_0 respectively. Here we take M_0 = 1236 MeV, Γ_0 = 120 MeV, and a = 1. Detailed discussions on the phenomenological analysis of resonances are in J. D. Jackson, Nuovo Cimento 36, 1644 (1964).

7. The $\chi^2 = \sum_{i=1}^{N} [N_D^i - N_{mc}^i)]$ where the N_D^i and the N_{mc}^i are the number of events from the data and the Monte Carlo calculation of the model in the ith bin of a distribution. Due to the statistical fluctuations we, in some cases, combine several bins into one.

8. Particle Data Group, Rev. Mod. Phys. 42, 87 (1970).

9. S. B. Treiman and C. N. Yang, Phys. Rev. Letters 8, 140 (1962).

10. H. Harari, Phys. Rev. Letters 20, 1395 (1968).

11. a) An earlier discussion was given by C. Fu, A. Firestone, G. Goldhaber, and G. H. Trilling in APS Washington Meeting, April 1969; Study of the $K\pi$ System in the Reaction $K^+p \to K^+\pi^-\Delta^{++}$ at 9 GeV/c; see also Ref. 1.

b) C. Fu, A. Firestone, G. Goldhaber, G. H. Trilling, and B. C. Shen, Lawrence Radiation Laboratory Report UCRL-18201 (1968).

12. Huan Lee, J. Math. Phys. 10, 779 (1969) and the references therein.

Table I. χ^2 values for sample B.[a]

Distribution	χ^2	d.f.[b]	Confidence level (%)	χ^2	d.f.[b]	Confidence level (%)
$M(K^+\pi^-)$	8.1	14	88.3	16.1	13	17.1
$M(\Delta^{++}\pi^-)$	18.3	11	7.3	15.2	10	12.5
$M(K^+\Delta^{++})$	8.7	9	46.4	10.8	8	21.5
$-t_{KK}$	20.8	6	0.2	11.4	5	4.4
$-t_{p\Delta}$	3.8	3	27.9	3.5	2	17.7
$-t_{K\pi}$	5.9	5	31.5	6.1	4	19.1
$-t_{p\pi}$	20.3	7	0.5	12.9	6	4.5
$\cos\theta(K^+\pi^-)$	22.2	12	3.5	12.9	11	29.4
$\phi(K^+\pi^-)$	23.3	17	14.1	19.6	16	23.9
$\cos\theta(\Delta^{++}\pi^-)$	32.3	15	0.6	19.3	14	15.3
$\phi(\Delta^{++}\pi^-)$	28.2	12	0.8	18.0	11	11.5
Toller angle ω	29.1	10	1.2	15.8	9	7.0

[a] See Ref. 6.

[b] Degrees of freedom.

Table II. Comparison of the number of events from the model and the phase space with the data under different kinematical criteria.

	$M(K^+\pi^-) \geq 1540$ MeV			$M(K^+\pi^-) < 1540$ MeV		
	Sample A	Sample B	Sample C	$-t_{KK}$ and $-t_{p\Delta} \leq 1.0$ (GeV/c)^2	$-t_{KK}$ and $-t_{p\Delta} < 0.5$ (GeV/c)^2	$-t_{KK}$ and $-t_{p\Delta} < 0.3$ (GeV/c)^2
Data	511	287	115	1804	1375	953
Case I	536	287	127	327	307	251
Case II	500	287	132	461	404	318
Phase space	1805	287	54	2565	824	330

FIGURE CAPTIONS

Fig. 1. A double-Regge-pole-exchange diagram for (a) a reaction $a + b \rightarrow 1 + 2 + 3$ and (b) the reactions $K^+p \rightarrow K^+\pi^-\Delta^{++}_{1236}$.

Fig. 2. Mass distributions for Δ^{++}_{1236} (1120 to 1320 MeV) for samples (a) A, (b) B, and (c) C. The solid curves show the distributions for Monte Carlo events.

Fig. 3. $K^+\pi^-$ mass distributions for samples (a) A, (b) B, and (c) C. The solid and the long-dash curves correspond to cases I and II respectively. The short-dash curves are the extrapolation of the cases I and II.

Fig. 4. $\Delta^{++}\pi^-$ mass distributions for samples (a) A, (b) B, and (c) C, and $K^+\Delta^{++}$ mass distributions for samples (d) A, (e) B, and (f) C. The solid and the long-dash curves, the results from the model, bear the same meaning as those shown in Fig. 3.

Fig. 5. $-t_{K^+K^+}$ distributions for samples (a) A, (b) B, and (c) C, and $-t_{p\Delta^{++}}$ distributions for samples (d) A, (e) B, and (f) C. The curves bear the same meaning as those shown in Fig. 4.

Fig. 6. $-t_{K^+\pi^-}$ distributions for samples (d) A, (e) B, and (f) C. The curves bear the same meaning as those shown in Fig. 4.

Fig. 7. $\cos\theta(K^+\pi^-)$ distributions for samples (a) A, (b) B, and (c) C and $\phi(K^+\pi^-)$ distributions for samples (d) A, (e) B, and (c) C. $\theta(K^+\pi^-)$ and $\phi(K^+\pi^-)$ are the Jackson angle and the Treiman-Yang angle for the $K^+\pi^-$ system. The curves bear the same meaning as those shown in Fig. 4.

Fig. 8. $\cos\theta(\Delta^{++}\pi^-)$ distributions for samples (a) A, (b) B, and (c) C and $\phi(\Delta^{++}\pi^-)$ distributions for samples (d) A, (e) B, and (f) C. $\theta(\Delta^{++}\pi^-)$ and $\phi(\Delta^{++}\pi^-)$ are the Jackson angle and the Treiman-Yang angle for the $\Delta^{++}\pi^-$ system. The curves bear the same meaning as those shown in Fig. 4.

Fig. 9. Toller angular distributions for samples (a) A, (b) B, and (c) C. The solid and the long-dash curves bear the same meaning as those shown in Fig. 4. The dash-dot curve indicates the phase space normalized to each sample.

Fig. 10. $K^+\pi^-$ mass distributions with $-t(K^+K^+)$ and $-t(p\Delta^{++})$ less than (a) 1.0 $(GeV/c)^2$, (b) 0.5 $(GeV/c)^2$, and (c) 0.3 $(GeV/c)^2$. The solid and the dashed curves bear the same meaning as those shown in Fig. 3.

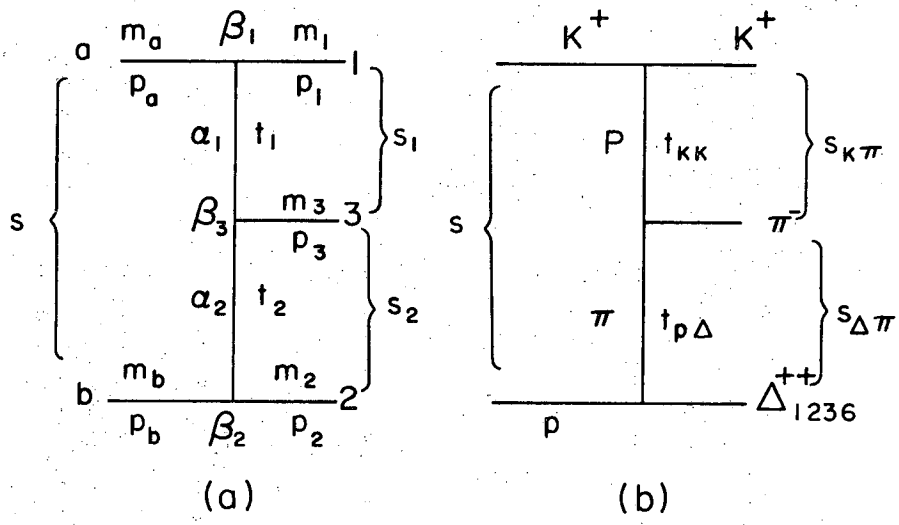

XBL703-2462

Fig. 1

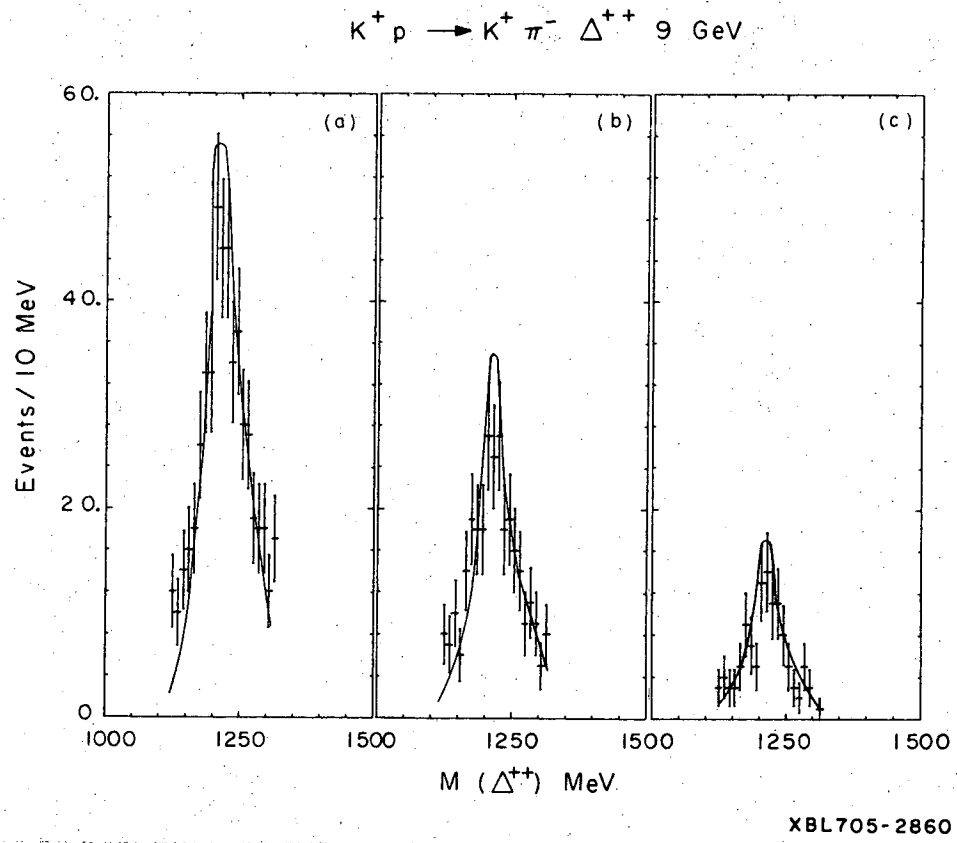

XBL705-2860

Fig. 2

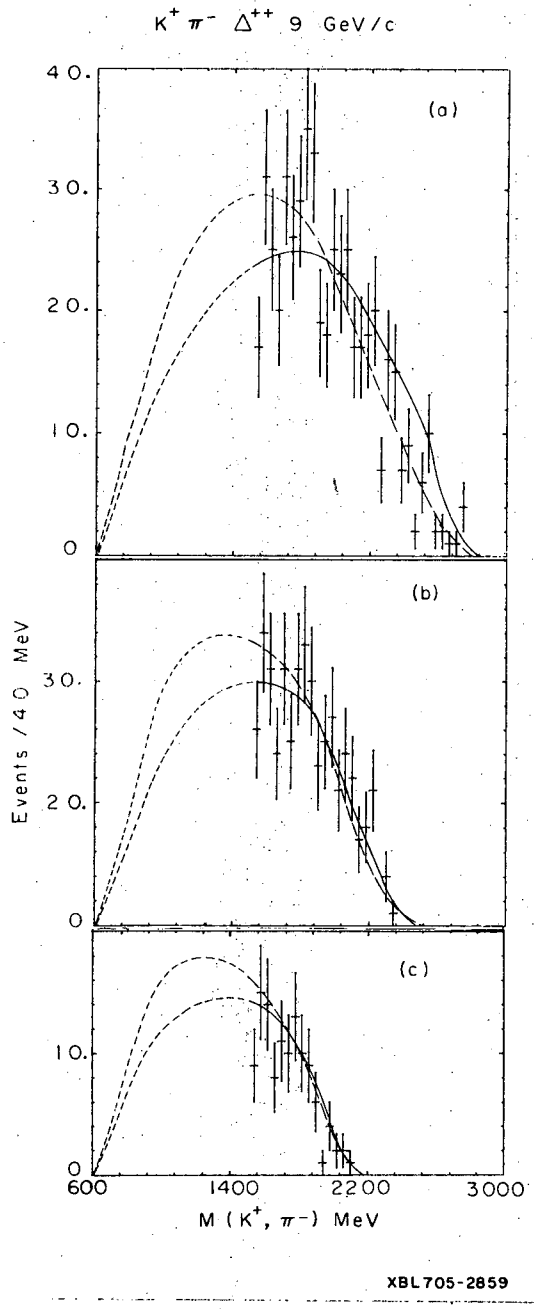
$K^+ \pi^- \Delta^{++}$ 9 GeV/c
(a)
(b)
(c)
Events / 40 MeV
M (K^+, π^-) MeV
XBL705-2859

Fig. 3

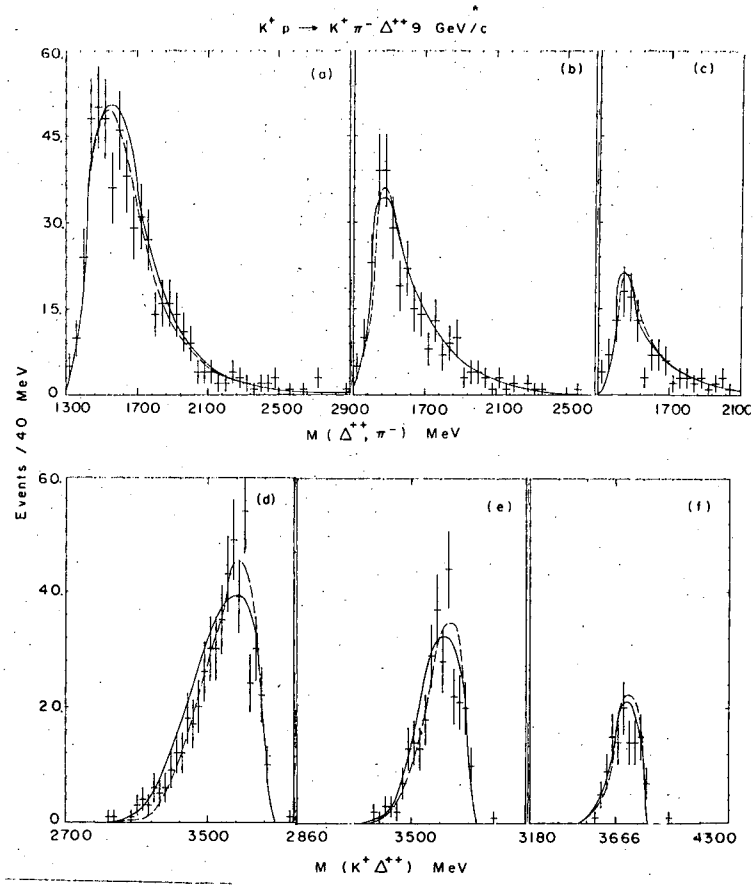
$K^+ p \rightarrow K^+ \pi^- \Delta^{++}$ 9 GeV/c
(a)
(b)
(c)
(d)
(e)
(f)
Events / 40 MeV
M (Δ^{++}, π^-) MeV
M ($K^+ \Delta^{++}$) MeV
XBL705-2855

Fig. 4

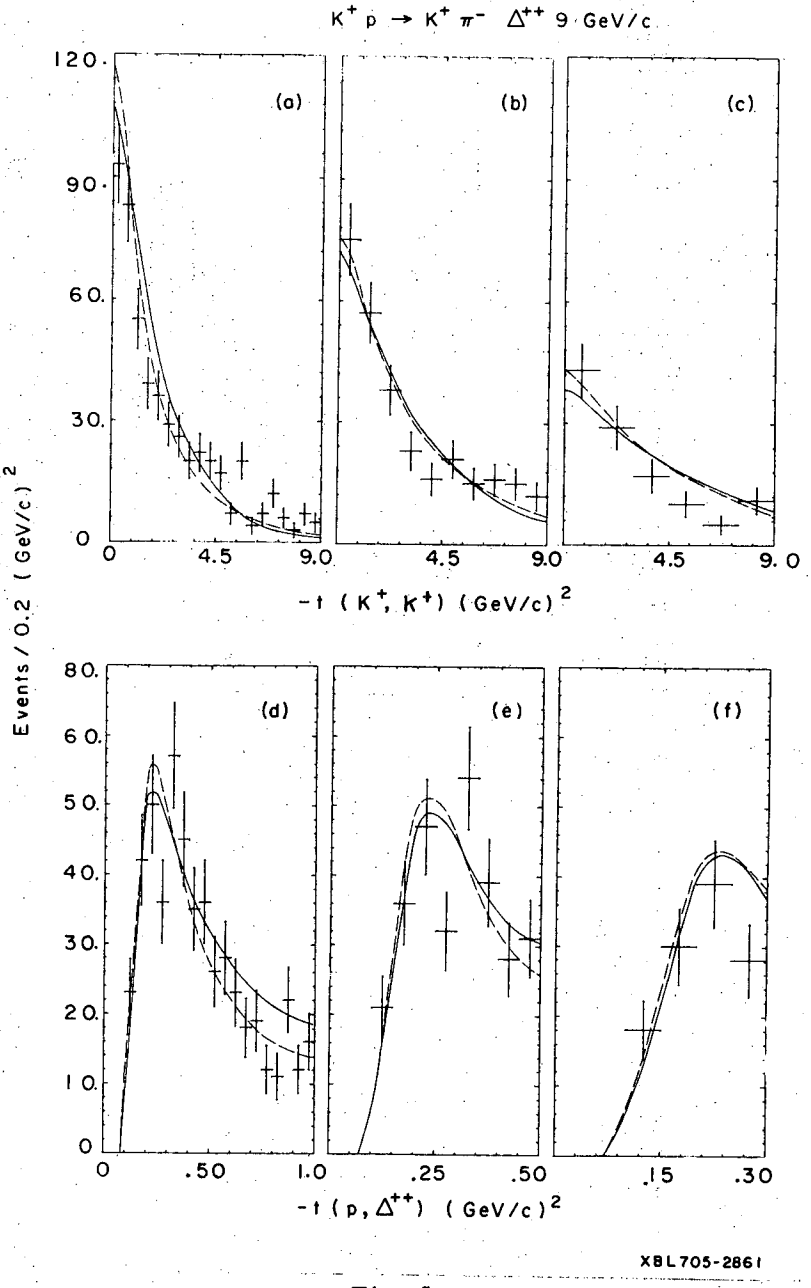
$K^+ p \to K^+ \pi^- \Delta^{++}$ 9 GeV/c
(a)
(b)
(c)
(d)
(e)
(f)
Events / 0.2 (GeV/c)^2
$-t\ (K^+, K^+)$ (GeV/c)^2
$-t\ (p, \Delta^{++})$ (GeV/c)^2
XBL705-2861

Fig. 5

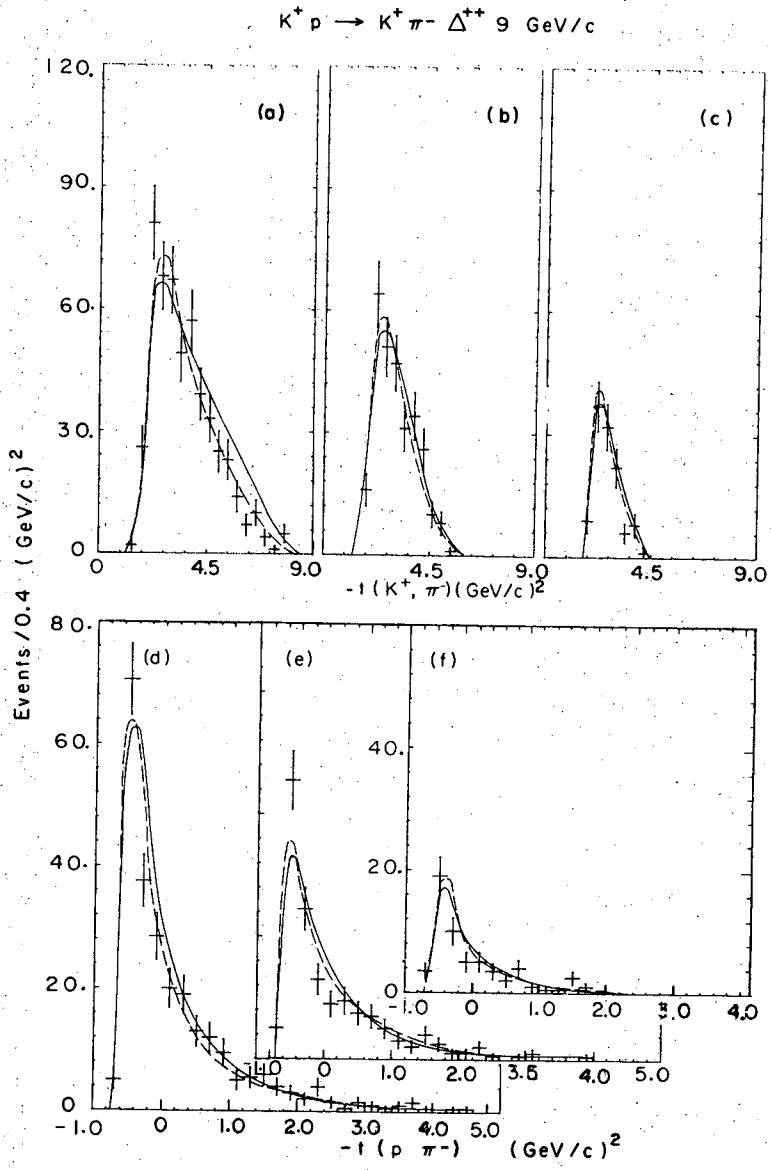

XBL705-2856

Fig. 6

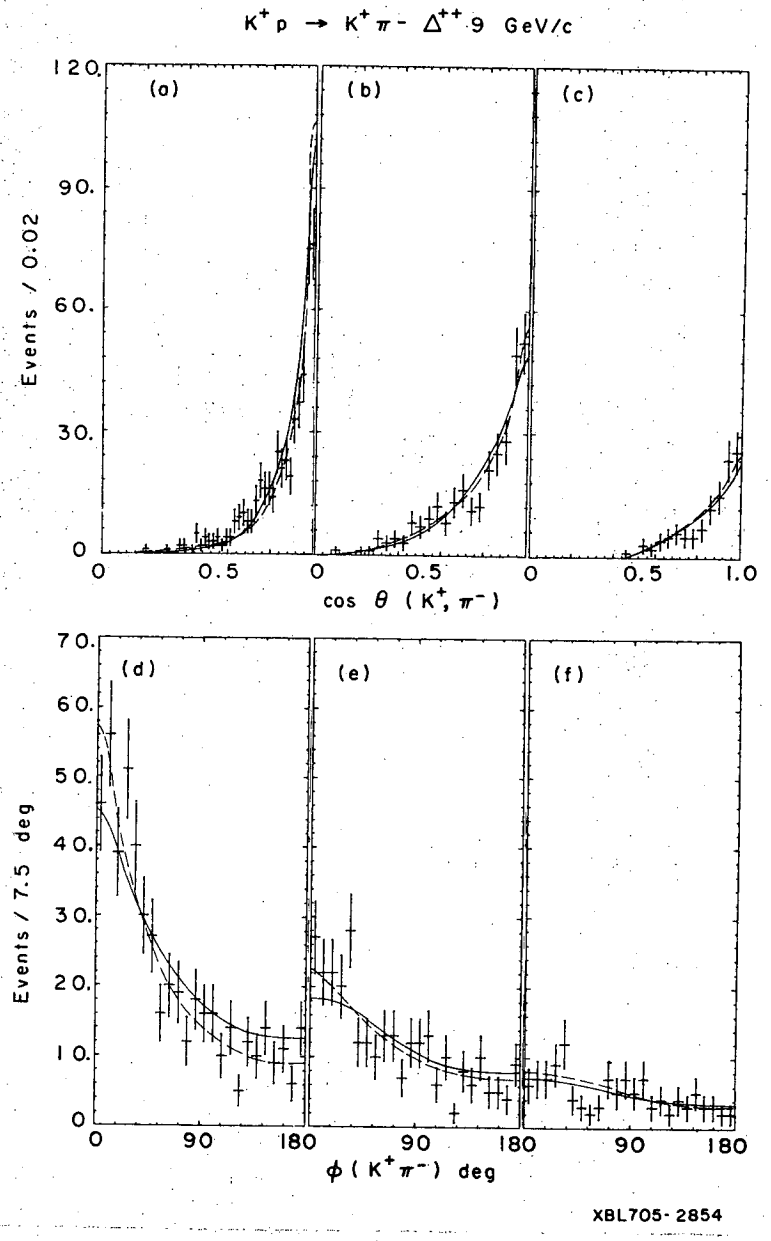
$K^+ p \rightarrow K^+ \pi^- \Delta^{++}$ 9 GeV/c
(a)
(b)
(c)
(d)
(e)
(f)
Events / 0.02
cos θ (K^+, π^-)
Events / 7.5 deg
φ ($K^+\pi^-$) deg
XBL705-2854

Fig. 7

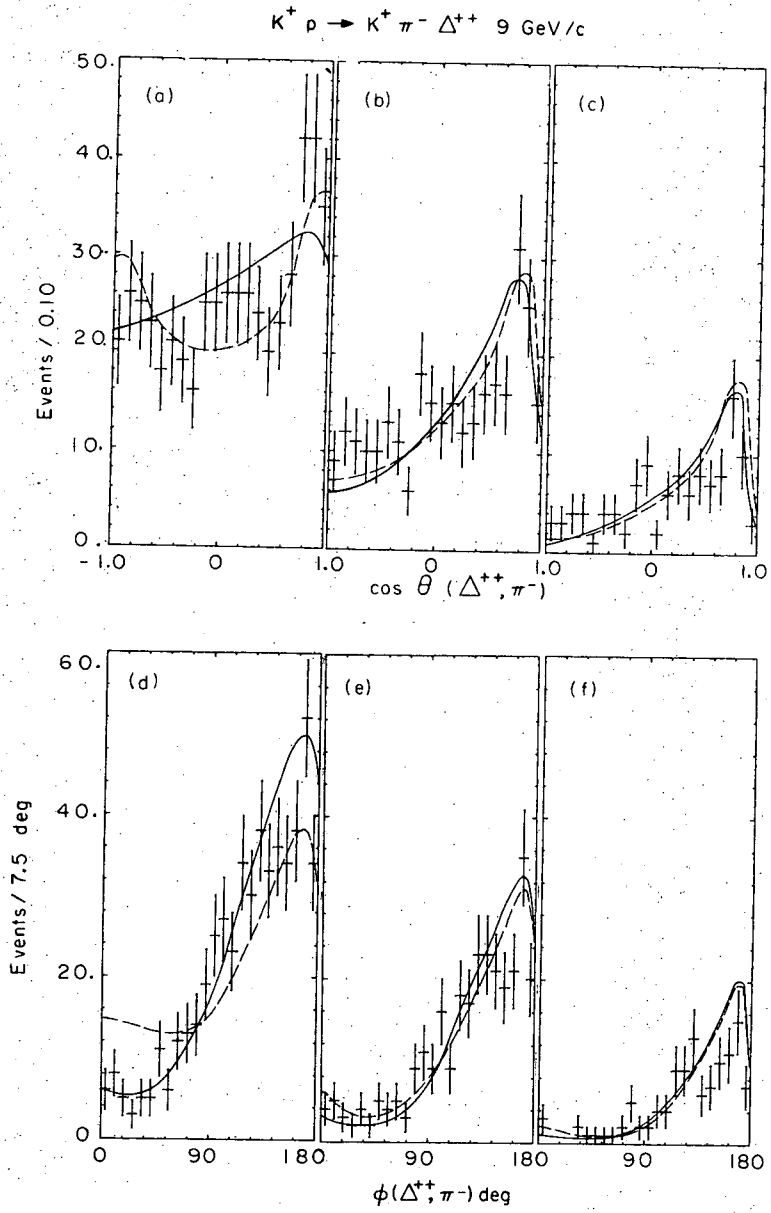
$K^+ p \rightarrow K^+ \pi^- \Delta^{++}$ 9 GeV/c
(a)
(b)
(c)
(d)
(e)
(f)
Events / 0.10
Events / 7.5 deg
cos θ (Δ^{++}, π^-)
ϕ(Δ^{++}, π^-) deg
XBL705-2857

Fig. 8

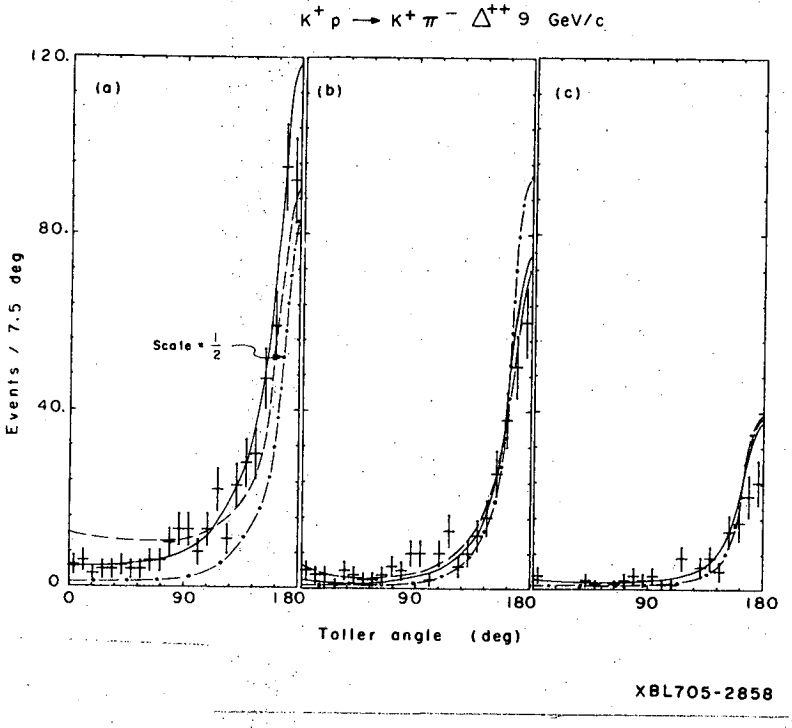
$K^+ p \rightarrow K^+ \pi^- \Delta^{++}$ 9 GeV/c
(a)
(b)
(c)
Scale = 1/2
Events / 7.5 deg
Toller angle (deg)
XBL705-2858

Fig. 9

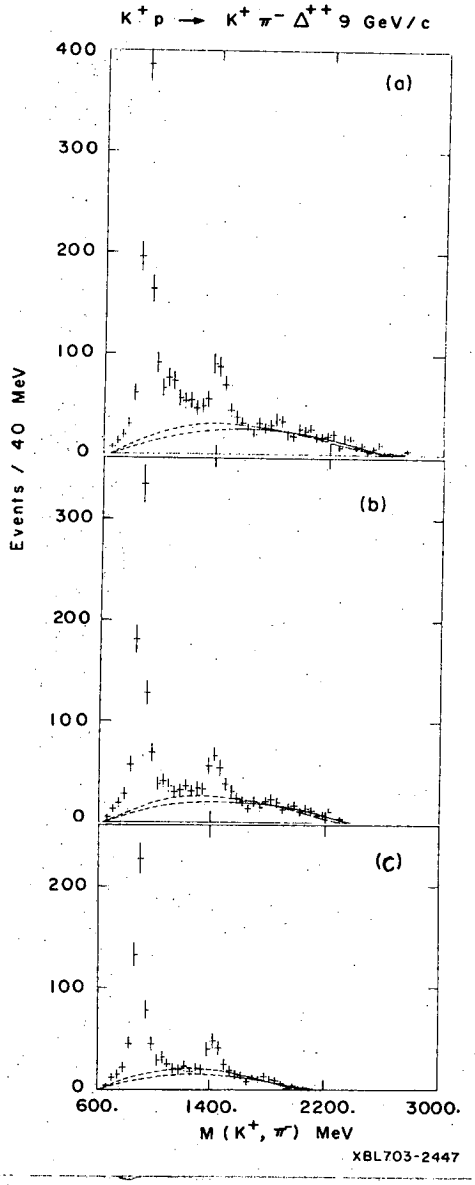
$K^+ p \rightarrow K^+ \pi^- \Delta^{++}$ 9 GeV/c
(a)
(b)
(c)
Events / 40 MeV
M (K^+, π^-) MeV
XBL703-2447

Fig. 10

TECHNICAL INFORMATION DIVISION
LAWRENCE RADIATION LABORATORY
UNIVERSITY OF CALIFORNIA
BERKELEY, CALIFORNIA 94720